

Element-Size Independent, Elasto-Plastic Damage Analysis of Framed Structures

Yutaka Toi and Keishi Hasegawa

Abstract— The adaptively shifted integration (ASI) technique and continuum damage mechanics are applied to the nonlinear finite element analysis of framed structures modeled by cubic Bernoulli-Euler beam elements. A new form of evolution equation of damage, which is a function of plastic relative rotational angles, is introduced in order to remove the mesh-dependence caused by the strain-dependence of damage. The elasto-plastic damage behavior of framed structures can be accurately and efficiently predicted by the combination of the ASI technique and the new damage evolution equation. Some numerical studies are carried out to show the mesh-independence of the proposed computational method.

Index Terms— Finite Element Method, Adaptively Shifted Integration Technique, Damage Mechanics, Framed Structures, Elasto-Plastic Damage Analysis, Cubic Bernoulli-Euler Beam Elements

I. INTRODUCTION

The occurrence and growth of a number of microscopic defects such as microcracks and microvoids in materials cause reduction of the stiffness, strength and toughness as well as the remaining life of materials. Continuum damage mechanics (abbreviated to CDM) is the theory that can take into account the effects of such microscopic defects on the mechanical properties of solids in the framework of continuum mechanics. CDM has been applied to the finite element analysis of various damage and failure problems of structural members in many literatures [1-5]. The so-called local approach to fracture based on damage mechanics and the finite element method can consistently model the mechanical behaviors from the initiation and evolution of damage through the propagation of macrocracks, however, it is pointed out as a problem that the calculated results considerably depend upon the assumed finite element mesh [3].

The damage analysis of framed structures based on CDM has been studied by many researchers [6-18]. Krajcinovic [6] defined the isotropic damage variable (the damage modulus) related to the fracture stress and used it to calculate the ultimate moment carrying capacities of concrete beams. Chandrakanth and Pandey [7] carried out the elasto-plastic damage analysis of Timoshenko layered beams. Cipollina et al. [8], Florez-Lopez [9], Thomson et al. [11], Perdomo et al. [12], Marante and Florez-Lopez [15], Marante et al. [17]

presented the formulation for the damage analysis of RC frames by the lumped dissipation model and implemented it in the commercial finite element program. Florez-Lopez [10] gave a unified formulation for the damage analysis of steel and RC frame members. Inghlessi et al. [13,14], and Febres et al. [16] conducted the analysis of steel frames considering damage and local buckling in tubular members. Addressi and Ciampi [18] proposed a new beam finite element based on damage mechanics and plasticity to analyze the cyclic structural response of plane frames. However, no discussion has been made for the mesh-dependence of the finite element solutions for the damage problem of framed structures in the existing literatures [6-18].

The cubic beam element based on Bernoulli-Euler hypothesis is generally used in the finite element analysis of framed structures neglecting the effect of shear deformation [19]. Toi [20] derived the relation between the location of a numerical integration point and the position of occurrence of a plastic hinge in the element, considering the equivalence condition for the strain energy approximations of the finite element and the computational discontinuum mechanics model composed of rigid bars and connection springs. The computational method identified as the adaptively shifted integration technique [21] (abbreviated to the ASI technique) was developed, based on this equivalence condition. The ASI technique, in which the plastic hinge can be formed at the exact position by adaptively shifting the position of a numerical integration point, gives accurate elasto-plastic solutions even by the modeling with the minimum number of elements. The ASI technique has been applied to the static and dynamic plastic collapse analysis of framed structures [21-24], through which the validity of the method has been demonstrated with respect to the computational efficiency and accuracy.

In the present study, a new computational method is formulated for the elasto-plastic damage analysis of framed structures, based on the ASI technique for the cubic Bernoulli-Euler beam element and the concept of CDM. The non-layered approach, in which the stress-strain relation is expressed in terms of the resultant stresses and the corresponding generalized strains, is employed in order to reduce the computing time for the large-scale framed structures. A new form of damage evolution equation, which is expressed in terms of the plastic relative rotational angles and the effective element length instead of the plastic curvature changes, is proposed in order to remove the mesh-dependence of solutions in the damage analysis. The present method is applicable to the collapse analysis of framed structures including elasto-plasticity, damage initiation, its evolution and fracture. Numerical studies for simple frames are conducted to show accuracy, efficiency and the mesh-independence of the proposed method.

Manuscript received August 9, 2011.

Y. Toi is with the Institute of Industrial Science, University of Tokyo, Komaba, Meguro-ku, Tokyo, 153-8505 Japan (phone: 03-5452-6178, fax: 03-5452-6180, e-mail: toi@iis.u-tokyo.ac.jp).

K. Hasegawa was with the Graduate School, University of Tokyo, Komaba, Meguro-ku, Tokyo, 153-8505 Japan.

II. ELASTO-PLASTIC DAMAGE ANALYSIS OF FRAMED STRUCTURES

A. ASI Technique

One of the authors Toi considered an equivalence condition for the strain energy approximations of the cubic Bernoulli-Euler beam element (the upper figure in Fig. 1) and the computational discontinuum mechanics model which is composed of rigid bars connected with the springs resisting relative rotational displacement (the lower figure in Fig. 1) [20]. The strain energy approximation of the cubic Bernoulli-Euler beam element is a function of the location of the numerical integration points s_i ($i = 1, 2$), while the strain energy function of the discontinuum mechanics model depends upon the position of the connection springs r_i ($i = 1, 2$). As a result, the following relation was obtained as the equivalence condition for both discrete models:

$$s_i = \mp \frac{1}{3r_2} \quad (i = 1, 2; r_1 = -r_2) \quad (1)$$

When the equivalence condition given by Eq. (1) is satisfied, the cubic Bernoulli-Euler beam element and the computational discontinuum mechanics model are completely the same.

The concept of plastic hinges can be easily, explicitly and accurately taken into account by reducing the rotational spring constant in the latter physical model. Therefore, it is clear that a plastic hinge can be formed at an arbitrary position in the cubic Bernoulli-Euler beam element by adaptively shifting the numerical integration points according to Eq. (1). When the integration points are located at $s_i = \mp 1/3$ ($i = 1, 2$), a plastic hinge is formed at either one of the edges or both as $r_i = \mp 1$ ($i = 1, 2$). This case is actually important when plastic hinges are formed at member joints or concentratedly loaded points, since they cannot be formed at exact positions when the numerical integration points are located at Gaussian integration points $s_i = \mp 1/\sqrt{3}$ ($i = 1, 2$) in each element as is usually done. The detailed computational procedure of the ASI technique is as follows.

The numerical integration points are located at Gaussian integration points $s_i = \mp 1/\sqrt{3}$ ($i = 1, 2$) while the element is entirely elastic. The incremental stiffness equation for the element is then given by

$$\mathbf{k} d\mathbf{u} = d\mathbf{f} \quad (2a)$$

where

$$\mathbf{k} = \frac{L_{elm}}{2} \left\{ \mathbf{B} \left(-\frac{1}{\sqrt{3}} \right)^t \mathbf{D}_e \left(-\frac{1}{\sqrt{3}} \right) \mathbf{B} \left(-\frac{1}{\sqrt{3}} \right) + \mathbf{B} \left(\frac{1}{\sqrt{3}} \right)^t \mathbf{D}_e \left(\frac{1}{\sqrt{3}} \right) \mathbf{B} \left(\frac{1}{\sqrt{3}} \right) \right\} \quad (2b)$$

In Eqs. (2a) and (2b), the following notations are used: \mathbf{k} ; the elastic element stiffness matrix, $d\mathbf{u}$; the nodal displacement increment vector, $d\mathbf{f}$; the nodal external force

increment vector, L_{elm} ; the element length, $\mathbf{B}(s_i)$; the generalized strain-nodal displacement matrix, $\mathbf{D}_e(r_i)$; the elastic resultant stress-generalized strain matrix. The generalized strain increment vector is calculated as

$$d\boldsymbol{\varepsilon} \left(\pm \frac{1}{\sqrt{3}} \right) = \mathbf{B} \left(\pm \frac{1}{\sqrt{3}} \right) d\mathbf{u} \quad (3)$$

The resultant stress increment vector is evaluated as

$$d\mathbf{R} \left(\pm \frac{1}{\sqrt{3}} \right) = \mathbf{D}_e \left(\pm \frac{1}{\sqrt{3}} \right) d\boldsymbol{\varepsilon} \left(\pm \frac{1}{\sqrt{3}} \right) \quad (4)$$

The distribution of resultant stresses in the elastically deformed element is determined by the following form of equation [21]:

$$d\mathbf{R}(s) = \mathbf{T}_1(s) d\mathbf{R} \left(-\frac{1}{\sqrt{3}} \right) + \mathbf{T}_2(s) d\mathbf{R} \left(\frac{1}{\sqrt{3}} \right) \quad (5)$$

where $\mathbf{T}_i(s)$ is the interpolation function matrix given in [21]. The location of the cross-section in the element which reaches a fully plastic state at first can be determined by comparing the calculated distribution of resultant stresses with the assumed yield function.

$$f[\mathbf{R}(r_2)] = \max_{-1 \leq s \leq 1} \{ f[\mathbf{R}(s)] \} \quad (6a)$$

or

$$f[\mathbf{R}(-r_2)] = \max_{-1 \leq s \leq 1} \{ f[\mathbf{R}(s)] \} \quad (6b)$$

Immediately after the occurrence of the fully plastic section, the numerical integration points are shifted to the new points ($s_i = \mp 1/3r_2$ ($i = 1, 2$)) according to Eq. (1) so as to form a plastic hinge exactly at the position of the fully plastic section. For instance, if a fully plastic section occurs at the right edge of the element ($r_2 = 1$), the numerical integration points are shifted to the points $s_i = \mp 1/3$ ($i = 1, 2$). The incremental stiffness equation at the following incremental step is then given by

$$\mathbf{k} d\mathbf{u} = d\mathbf{f} \quad (7a)$$

where

$$\mathbf{k} = \frac{L_{elm}}{2} \left\{ \mathbf{B} \left(-\frac{1}{3r_2} \right)^t \mathbf{D}_e(-r_2) \mathbf{B} \left(-\frac{1}{3r_2} \right) + \mathbf{B} \left(\frac{1}{3r_2} \right)^t \mathbf{D}_{epd}(r_2) \mathbf{B} \left(\frac{1}{3r_2} \right) \right\} \quad (7b)$$

In Eq. (7b), $\mathbf{D}_{epd}(r_1)$ is the resultant stress-generalized strain matrix for the elasto-plastic deformation considering damage. The generalized strain increment vector is calculated as

$$d\boldsymbol{\varepsilon}(\pm r_2) = \mathbf{B} \left(\pm \frac{1}{3r_2} \right) d\mathbf{u} \quad (8)$$

The resultant stress increment vector is evaluated as

$$d\mathbf{R}(r_2) = \mathbf{D}_{epd}(r_2) d\boldsymbol{\varepsilon}(r_2) \quad (9a)$$

$$d\mathbf{R}(-r_2) = \mathbf{D}_e(-r_2) d\boldsymbol{\varepsilon}(-r_2) \quad (9b)$$

The numerical integration points return to the Gaussian integration points when the unloading occurs, and they are shifted again after reyielding.

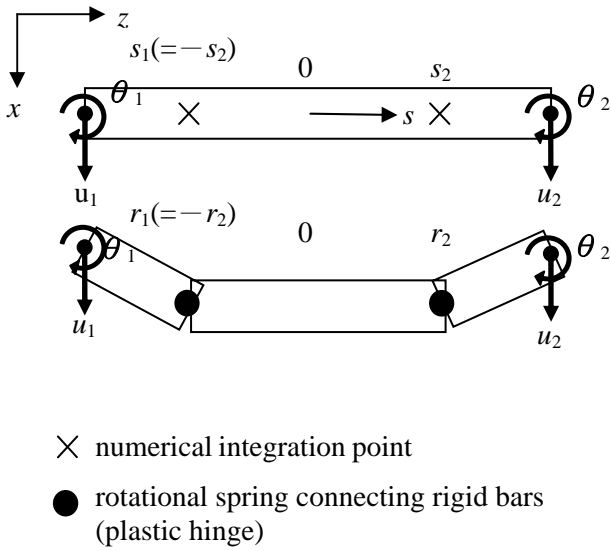


Fig.1 Cubic Bernoulli-Euler beam element and its physical equivalent

B. Elasto-Plastic Damage Constitutive Equation

The elasto-plastic damage constitutive equation is formulated for the incremental analysis of framed structures in the present section, based on the previous study for the elasto-plastic analysis of framed structures by the non-layered approach [25] and the concept of CDM [1].

The dissipation potential of the system is the sum of the plastic potential and the damage potential, which is given by the following equation:

$$F = F_p(\bar{\mathbf{R}}, R; D) + F_D(Y; r, D) \quad (10)$$

where F_p is the plastic potential for the evolution of plastic strains that is a function of the effective resultant stress ($\bar{\mathbf{R}}$), the isotropic hardening stress variable (R) and the scalar damage variable (D). F_D is the damage potential for the evolution of damage that is a function of the strain energy density release rate (Y), the strain of isotropic hardening (r) and the scalar damage variable (D).

The damage increment is obtained by the following equation:

$$dD = d\lambda \frac{\partial F}{\partial Y} = d\lambda \frac{\partial F_D}{\partial Y} \quad (11)$$

where $d\lambda$ is a proportional coefficient. The concrete form of this equation is discussed in the next section.

The yield function is assumed as follows:

$$f = \bar{\sigma}_{eq} - R - \sigma_0 = 0 \quad (12)$$

where the equivalent effective stress $\bar{\sigma}_{eq}$ is given as follows:

$$\bar{\sigma}_{eq}^2 = \left(\frac{\bar{R}_1}{Z_{x0}}\right)^2 + \left(\frac{\bar{R}_2}{Z_{y0}}\right)^2 + \left(\frac{\bar{R}_3}{A}\right)^2 + \left(\frac{\bar{R}_4}{W_p}\right)^2 \quad (13)$$

in which R_1, R_2, R_3 and R_4 are the two components of bending moments, the axial force and the torsional moment respectively. A is the cross-sectional area. Z_{x0}, Z_{y0} and W_p are the plastic sectional factors [26]. Each effective

resultant stress component is given by the following equation:

$$\bar{R}_i = R_i / (1 - D) \quad (i = 1, \dots, 4) \quad (14)$$

The following equation is assumed to hold on the yield surface considering damage:

$$df = \frac{\partial f}{\partial \bar{\mathbf{R}}} d\bar{\mathbf{R}} + \frac{\partial f}{\partial R} dR + \frac{\partial f}{\partial D} dD = 0 \quad (15)$$

Using the yield function of Eq. (12) as the plastic potential F_p in Eq. (10), the generalized plastic strain increment ($d\epsilon_p$) and the strain increment of isotropic hardening (dr) are given by the following equations:

$$d\epsilon_p = d\lambda \frac{\partial F}{\partial \bar{\mathbf{R}}} = d\lambda \frac{\partial F_p}{\partial \bar{\mathbf{R}}} \quad (16)$$

$$dr = -\frac{d\lambda \frac{\partial F}{\partial R}}{A \frac{\partial F}{\partial R}} = -\frac{d\lambda \frac{\partial F_p}{\partial R}}{A \frac{\partial F}{\partial R}} \quad (17)$$

where $d\lambda$ is a proportional coefficient.

The total strain increment in the plastic state is the sum of the elastic strain increment and the plastic strain increment. As a result, the following equation is obtained:

$$d\bar{\mathbf{R}} = \mathbf{D}_e d\epsilon_e = \mathbf{D}_e (d\epsilon - d\epsilon_p) = \mathbf{D}_e d\epsilon - \mathbf{D}_e d\lambda \frac{\partial F_p}{\partial \bar{\mathbf{R}}} \quad (18)$$

where \mathbf{D}_e is the elastic resultant stress-generalized strain matrix. $d\epsilon_e$ and $d\epsilon_p$ are the generalized elastic and plastic strain increment respectively.

The plastic hardening parameter and its increment are assumed as follows:

$$R = Kr^n \quad (19)$$

$$dR = nKr^{n-1} dr = Hdr = H \frac{d\lambda}{A} \quad (20)$$

where K and n are the material constants.

Substituting Eqs. (11), (12), (16) (18) and (20) into Eq. (15), the proportional coefficient $d\lambda$ is calculated as follows:

$$d\lambda = \frac{\left(\frac{\partial F_p}{\partial \bar{\mathbf{R}}}\right)^T \mathbf{D}_e}{\frac{H}{A} + \left(\frac{\partial F_p}{\partial \bar{\mathbf{R}}}\right)^T \mathbf{D}_e \frac{\partial F_p}{\partial \bar{\mathbf{R}}} + \frac{\bar{\sigma}_{eq}}{1-D} \frac{\partial F_D}{\partial Y}} d\epsilon \quad (21)$$

Substituting Eq. (21) into (18), the following incremental relation between effective resultant stresses and generalized strains can be obtained:

$$d\bar{\mathbf{R}} = \bar{\mathbf{D}}_{epd} d\epsilon = \mathbf{D}_e \left[1 - \frac{\frac{\partial F_p}{\partial \bar{\mathbf{R}}} \left(\frac{\partial F_p}{\partial \bar{\mathbf{R}}}\right)^T \mathbf{D}_e}{\frac{H}{A} + \left(\frac{\partial F_p}{\partial \bar{\mathbf{R}}}\right)^T \mathbf{D}_e \frac{\partial F_p}{\partial \bar{\mathbf{R}}} + \frac{\bar{\sigma}_{eq}}{1-D} \frac{\partial F_D}{\partial Y}} \right] d\epsilon \quad (22)$$

where $\bar{\mathbf{D}}_{epd}$ is the tangential, elasto-plastic damage stiffness matrix.

The incremental relation between resultant stresses and generalized strains is given by the following equation:

$$d\mathbf{R} = (1 - D)d\bar{\mathbf{R}} - \bar{\mathbf{R}}dD = \mathbf{D}_{epd} d\epsilon$$

$$= \left[(1-D)\mathbf{D}_e - \left\{ (1-D)\mathbf{D}_e \frac{\partial F_p}{\partial \mathbf{R}} + \bar{\mathbf{R}} \frac{\partial F_d}{\partial Y} \right\} \frac{\left(\frac{\partial F_p}{\partial \mathbf{R}} \right)^T \mathbf{D}_e}{\frac{H}{A} + \left(\frac{\partial F_p}{\partial \mathbf{R}} \right)^T \mathbf{D}_e \frac{\partial F_p}{\partial \mathbf{R}} + \frac{\bar{\sigma}_{eq}}{1-D} \frac{\partial F_d}{\partial Y}} \right] d\boldsymbol{\varepsilon} \quad (23)$$

where \mathbf{D}_{epd} is the tangential, elasto-plastic damage matrix relating resultant stress increments with generalized strain increments to be used in Eqs. (7b) and (9a).

C. Damage Evolution Equation

The following damage evolution equation given by Lemaitre [1] is used as Eq. (11) in the preceding section:

$$dD = \left(\frac{Y}{S} \right)^s dp \quad \text{when } p \geq p_D \quad (24a)$$

where

$$dp = \frac{dr}{1-D} \quad (24b)$$

S and s in Eq. (24a) are material constants. p and p_D are the accumulated equivalent generalized plastic strain and its critical value for the initiation of damage. The equivalent generalized plastic strain increment $dp(\boldsymbol{\kappa})$ is given as follows:

$$dp(\boldsymbol{\kappa}) = \frac{d\lambda}{A(1-D)} \propto \frac{\bar{R}_1}{Z_{x0}^2} EI_x d\boldsymbol{\kappa}_x + \frac{\bar{R}_2}{Z_{y0}^2} EI_y d\boldsymbol{\kappa}_y + \frac{\bar{R}_3}{A^2} EAd\varepsilon + \frac{\bar{R}_4}{W_p^2} GA d\theta_z' \quad (25)$$

where $d\boldsymbol{\kappa}_x$ and $d\boldsymbol{\kappa}_y$ are the curvature change increments. $d\varepsilon$ and $d\theta_z'$ are the average axial strain and the torsional rate respectively. The notation $dp(\boldsymbol{\kappa})$ indicates that the equivalent generalized plastic strain increment dp is a function of curvature changes here. The strain energy release rate Y is given as follows:

$$Y = \frac{\sigma_{eq}^2}{2E(1-D)^2} \quad (26)$$

where E is Young's modulus. The time-independent damage that evolves with an increase of the equivalent stress and the equivalent plastic strain is assumed in the present analysis.

The generalized strain increment in the elasto-plastic behavior is the sum of the elastic component and the plastic component. Therefore the relation with the nodal displacement increment is expressed by the following equation:

$$d\boldsymbol{\varepsilon}_e + d\boldsymbol{\varepsilon}_p = \mathbf{B}(d\mathbf{u}_e + d\mathbf{u}_p) \quad (27)$$

The relation between the curvature change increment and the nodal displacement increment for the cubic Bernoulli-Euler beam element is given by the following equation:

$$d\boldsymbol{\kappa}_x^e + d\boldsymbol{\kappa}_x^p = \left(\frac{2}{L_{elm}^2} du_1^e - \frac{2}{L_{elm}^2} du_2^e - \frac{2}{L_{elm}} d\theta_{x2}^e \right) + \left(\frac{2}{L_{elm}^2} du_1^p - \frac{2}{L_{elm}^2} du_2^p - \frac{2}{L_{elm}} d\theta_{x2}^p \right) \quad (28)$$

where L_{elm} is the element length. The superscripts e and p indicate an elastic and a plastic component respectively. The subscripts 1 and 2 indicate nodes at both edges of the element. The plastic relative rotational angle $d\theta^p$ at the plastic hinge can be accurately calculated by the application of the ASI technique, not depending on the element length. This can be proved by the fact that the plastic collapse load of framed structures calculated by the ASI technique coincides with the exact solution given by the theoretical plastic analysis [26], independent of the number of elements [21]. On the other hand, the calculated curvature changes are mesh-dependent.

The damage evolution calculated by Eqs. (24), (25) and (26) extremely depends on the element length (L_{elm}) since the damage evolution equation is expressed in terms of the curvature change increments as shown in Eq. (25). Then, Eq. (25) is replaced with the following equation:

$$dp(\bar{\theta}) = \frac{d\lambda}{A(1-D)} \propto \frac{\bar{R}_1}{Z_{x0}^2} EI_x \frac{2d\bar{\theta}_x^p}{L_{eff,x}} + \frac{\bar{R}_2}{Z_{y0}^2} EI_y \frac{2d\bar{\theta}_y^p}{L_{eff,y}} + \frac{\bar{R}_3}{A^2} EAd\varepsilon + \frac{\bar{R}_4}{W_p^2} GA d\theta_z' \quad (29)$$

where

$$d\bar{\theta}_x^p = \left(\frac{1}{L_{elm}} du_1^p - \frac{1}{L_{elm}} du_2^p - d\theta_{x2}^p \right) \quad (30)$$

$$d\bar{\theta}_y^p = \left(\frac{1}{L_{elm}} dv_1^p - \frac{1}{L_{elm}} dv_2^p - d\theta_{y2}^p \right)$$

In Eq. (29), $L_{eff,x}$ and $L_{eff,y}$ are the effective element length dependent on the shape and dimension of the cross-section and the material property, which are the parameters relating the curvature change increments with the plastic relative rotational angles $d\bar{\theta}_x^p$ and $d\bar{\theta}_y^p$. The elastic relative rotational angles are neglected here as their effects can generally be considered to be small. It is assumed in Eq. (30) that a plastic hinge is formed at the right edge of the element. The plastic relative rotational angle is an important parameter in the plastic analysis of framed structures [26], in which the plastic collapse load and the residual strength of plastic hinges are calculated and discussed by using this parameter. The effective element length as well as the other material constants concerning damage should be determined in the experiments containing bending tests of frame members. However, the tentative values are used in numerical examples in the next chapter. It is expected that the use of $dp(\bar{\theta})$ in Eq. (29) instead of $dp(\boldsymbol{\kappa})$ in Eq. (25) will remove the mesh-dependence of the finite element solutions for the elasto-plastic damage analysis of framed structures.

III. NUMERICAL EXAMPLES

The elasto-plastic damage analysis of a simple space frame is conducted in the present section. Figure 2 shows the

loading condition, the boundary condition and the plastic hinges with their sequence to be formed in the space frame. The space frame is fixed at lower ends and subjected to a concentrated load horizontally. The material constants, the dimensions and the damage parameters for the space frame are assumed as follows: $E = 210$ [GPa], $E_t = 0$ [GPa], $\sigma_0 = 300$ [MPa], $L = 710$ [mm], $B = 10$ [mm], $H = 10$ [mm], $S = 0.003$ [MPa], $s = 1$ and $p_D = 0.001$. Each member is uniformly subdivided with one, two, four, eight and sixteen elements. The element length in the case when each member is uniformly subdivided with sixteen elements is tentatively used as the effective element length $L_{eff,x}$ and $L_{eff,y}$.

Figure 3 shows the results calculated by the conventional finite element method (not using the ASI technique) which employs the damage evolution equation expressed in terms of the equivalent plastic strain increment $dp(\kappa)$ given by Eq. (25). The numerical integration points in each element are always located at Gaussian integration points through the whole deformation process, therefore a plastic hinge considering damage can be formed only at Gaussian integration points in each element. Consequently, the convergence of solutions for the plastic collapse load and the damage softening behavior is very slow, although the solutions are improved with the mesh refinement.

When applying the ASI technique to the analysis of Fig. 3, the calculated plastic collapse loads are completely independent of the element subdivision as shown in Fig. 4, because the locations of formation of plastic hinges, which are member joints in this problem, are exactly considered in the present analysis. However, the convergence of solutions after the occurrence of damage is still slow, as the damage evolution is calculated by using the equivalent plastic strain increment $dp(\kappa)$ given as a function of the curvature change increment.

Figures 5 shows the results calculated by the finite element method using the ASI technique based on the damage evolution equation expressed in terms of the equivalent plastic strain increment $dp(\theta)$ given in Eq. (29). As shown in this figure, the mesh-dependence has almost been removed and the highest computational efficiency and accuracy have been achieved by the combined use of the ASI technique and the new damage evolution equation expressed in terms of the plastic relative rotational angles. It can be concluded that one-element modeling per member is practically possible for the elasto-plastic damage analysis of space framed structures using cubic beam elements based on Bernoulli-Euler hypothesis.

The converged solution depends on the values of the effective element length $L_{eff,x}$ and $L_{eff,y}$ influenced by the shape and dimension of the cross-section and the material property, which should practically be determined by the bending tests for a limited number of typical member joints in the large-scale framed structure to be analyzed. Once they

have been experimentally determined, they can be introduced in the elasto-plastic damage analysis of the large-scale framed structures.

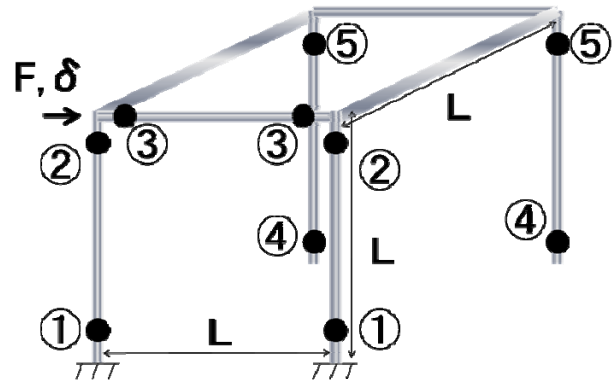


Fig.2 Space frame under lateral loading
 (• : plastic hinge)

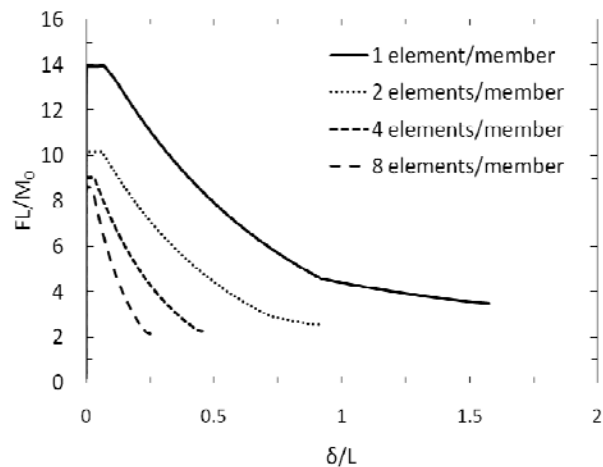


Fig.3 Load-deflection curves for a space frame by the conventional method using $dp(\kappa)$

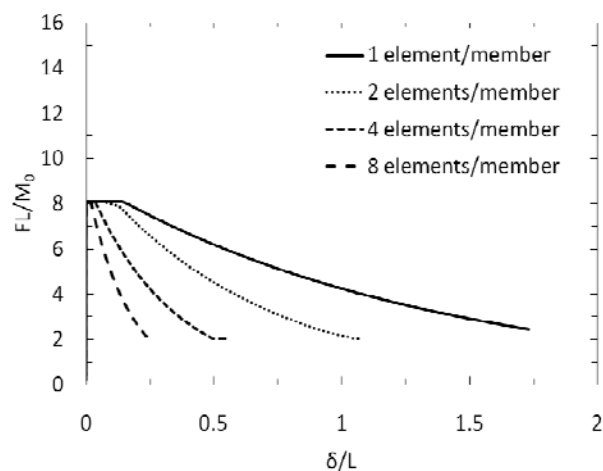


Fig.4 Load-deflection curves for a space frame by the ASI technique using $dp(\kappa)$

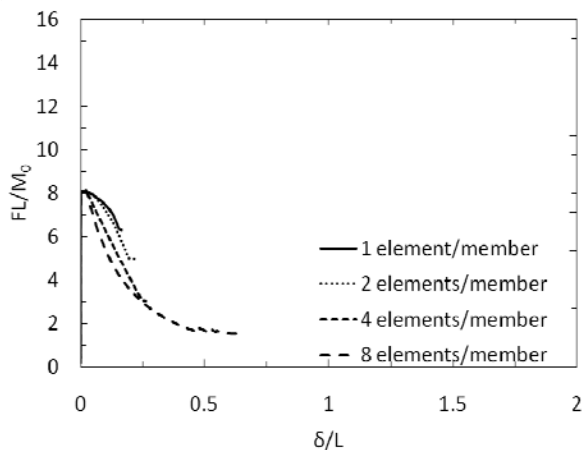


Fig.5 Load-deflection curves for a space frame by the ASI technique using $dp(\bar{\theta})$

IV. CONCLUSION

A new finite element formulation for the elasto-plastic damage analysis of framed structures has been proposed by the combined use of the ASI technique for cubic Bernoulli-Euler beam elements and the new damage evolution equation expressed in terms of plastic relative rotational angles. It has been confirmed through some numerical studies that the present method is almost mesh-independent and one-element idealization per member is possible for practical purposes. The present computational method can analyze the collapse behavior of large-scale framed structures considering elasto-plasticity, damage and fracture with the highest computational efficiency and accuracy. Furthermore, the present algorithm can easily be implemented in the existing finite element program. The tentative value was used as the effective element length for the present numerical studies, which should more exactly be determined by the bending tests or the plate/shell level finite element analysis of typical member joints in the framed structure to be analyzed.

REFERENCES

[1] Lemaitre, J., *A Course on Damage Mechanics*, Second Edition, (1996), Springer.
[2] Krajcinovic, D., *Damage Mechanics*, (1996), Elsevier.
[3] Skrzypek, J. and Ganczarski, A., *Modeling of Material Damage and Failure of Structures: Theory and Applications*, (1999), Springer.
[4] Kattan, P. I. and Voyiadjis, G. Z., *Damage Mechanics with Finite Elements*, (2001), Springer.
[5] Lemaitre, J. and Desmorat, R. *Engineering Damage Mechanics*, (2005), Springer.
[6] Krajcinovic, D., Distributed Damage Theory of Beams in Pure Bending, *Journal of Applied Mechanics*, Transactions of ASME, 46 (1979), pp.592-596.
[7] Chandrakanth, S. and Pandey, P. C., Damage Coupled Elasto-Plastic Finite Element Analysis of a Timoshenko Layered Beam, *Computers and Structures*, 69 (1988), pp.411-420.
[8] Cipollina, A. et al., A Simplified Damage Mechanics Approach to Nonlinear Analysis of Frames, *Computers and Structures*, 54(6) (1995), pp.1113-1126.
[9] Florez-Lopez, J., Simplified Model of Unilateral Damage for RC

Frames, *J. of Structural Engineering-ASCE*, 121(12) (1995), pp.1765-1772.
[10] Florez-Lopez, J., Frame Analysis and Continuum Damage Mechanics, *European Journal of Mechanics A/Solids*, 17(2) (1998), pp.269-283.
[11] Thomson, E. et al., Simplified Model of Low Cycle Fatigue for RC Frames. *Journal of Structural Engineering-ASCE*, 124(9) (1998), pp.1082-1085.
[12] Perdomo, M. E. et al., Simulation of Damage in RC Frames with Variable Axial Forces, *Earthquake Engineering & Structural Dynamics*, 28(3) (1999), pp.311-328.
[13] Inglessis, P. et al., Model of Damage for Steel Frame Members. *Engineering Structures*, 21(10) (1999), pp.954-964.
[14] Inglessis, P. et al., Modeling of Local Buckling in Tubular Steel Frames by Using Plastic Hinges with Damage, *Steel & Composite Structures*, 2(1) (2002), pp.21-34.
[15] Marante, M. E. and Florez-Lopez, J., Three-Dimensional Analysis of Reinforced Concrete Frames Based on Lumped Damage Mechanics, *International Journal of Solids and Structures*, 40(19) (2003), pp.5109-5123.
[16] Febres, R. et al., Modeling of Local Buckling in Tubular Steel Frames Subjected to Cyclic Loading, *Computers and Structures*, 81(22-23) (2003), pp.2237-2247.
[17] Marante, M. E. et al., Portal of Damage: A Web-Based Finite Element Program for the Analysis of Framed Structures Subjected to Overloads, *Advances in Engineering Software*, 36 (2005), pp.346-358
[18] Addressi, D. and Ciampi, V., A Regularized Force-Based Beam Element with a Damage-Plastic Section Constitutive Law, *International Journal for Numerical Methods in Engineering*, 70 (2007), pp.610-629.
[19] Bathe, K. J., *Finite Element Procedures*, (1996), Prentice Hall.
[20] Toi, Y., Shifted Integration Technique in One-Dimensional Plastic Collapse Analysis Using Linear and Cubic Finite Elements, *International Journal for Numerical Methods in Engineering*, 31 (1991), pp.1537-1552.
[21] Toi, Y. and Isobe, D., Adaptively Shifted Integration Technique for Finite Element Collapse Analysis of Framed Structures, *International Journal for Numerical Methods in Engineering*, 36 (1993), pp.2323-2339.
[22] Toi, Y. and Isobe, D., Finite Element Analysis of Quasi-Static and Dynamic Collapse Behaviors of Framed Structures by the Adaptively Shifted Integration Technique, *Computers and Structures*, 58 (1996), pp.947-955.
[23] Toi, Y. and Lee, J. G., Finite Element Crash Analysis of Framed Structures by the Adaptively Shifted Integration Technique, *JSME International Journal*, Series A 43(3) (2000), pp.242-251.
[24] Isobe, D. and Toi, Y., Analysis of Structurally Discontinuous Reinforced Concrete Building Frames Using the ASI Technique, *Computers and Structures*, 76(4) (2000), pp.242-251.
[25] Toi, Y. and Yang, H. J., Finite Element Crush Analysis of Framed Structures, *Computers and Structures*, 41(1) (1991), pp.137-149.
[26] Hodge Jr., P. G., *Plastic Analysis of Structures*, (1959), McGraw-Hill.